

# RESEARCH ACTIVITIES IV

## Department of Molecular Assemblies

### IV-A Solid State Properties of Phthalocyanine Salts and Related Compounds

Some phthalocyanine molecules contain unpaired d-electrons in the conjugated  $\pi$ -electron system. Due to this special nature, the itinerant  $\pi$ -electrons and localized unpaired d-electrons coexist in solid phthalocyanine salts, in which a one-dimensional double-chain system (metal and ligand chain) is formed. Furthermore these chains make up wide ( $\pi$ -band) and narrow (d-band) one-dimensional bands, the energy of the narrow band being close to the Fermi energy of the wide band. The phthalocyanine conductor is thus a two-chain and two-band system. The exchange interaction of itinerant  $\pi$ -electrons with localized magnetic moments is a new aspect in the field of organic metals. For the sake of basic understanding of these materials, where a magnetic interaction takes an important role, we prepare and characterize the solid phthalocyanine salts and related compounds.

#### IV-A-1 ESR Properties of Oriented Single Crystals of $\text{Co}_x\text{Ni}_{1-x}\text{Pc}(\text{AsF}_6)_{0.5}$

SIMONYAN, Mkhitar; YONEHARA, Yukako<sup>1</sup>;  
DING, Yuqin<sup>1</sup>; YAKUSHI, Kyuya  
(<sup>1</sup>GUAS)

Phthalocyanine conductor  $\text{CoPc}(\text{AsF}_6)_{0.5}$  has two magnetic subsystems: the localized 3d-electron of Co and itinerant  $\pi$ -electron of Pc. However, this compound is ESR silent, since the spin-orbit interaction in Co and dipole-dipole interaction between molecules are strong. The magnetically diluted system  $\text{Co}_x\text{Ni}_{1-x}\text{Pc}(\text{AsF}_6)_{0.5}$  is formed by mixing  $\text{CoPc}(\text{AsF}_6)_{0.5}$  in non-magnetic nearly isostructural  $\text{NiPc}(\text{AsF}_6)_{0.5}$ . When  $x = 0.01$ , we found an anisotropic hyperfine structure at 3.2 K. From the angular dependence of the hyperfine structure, the hyperfine constants and principal  $g$ -values are determined as  $A = 0.017 \text{ cm}^{-1}$ ,  $B = 0.032 \text{ cm}^{-1}$ ,  $g_{\parallel} = 2.056$ , and  $g_{\perp} = 3.045$  at 3.2 K. The hyperfine constants  $A$  and  $B$  are very close to those of insulating mixed crystal  $\text{Co}_{0.001}\text{Ni}_{0.999}\text{Pc}$  but the  $g$ -values are very different between them, which means the different electronic state in Co 3d-orbital. In contrast to  $\text{Co}_{0.001}\text{Ni}_{0.999}\text{Pc}$ , the ESR signal of  $\text{Co}_{0.01}\text{Ni}_{0.99}\text{Pc}(\text{AsF}_6)_{0.5}$  shows strong temperature dependence. As shown in Figure 1, the hyperfine structure collapse into a single Lorentzian line above 40 K, the metal-insulator transition temperature. This is direct evidence that the conduction electrons in ligand (Pc) site are interacting with the local magnetic moment of Co site. This exchange interaction is strongly reflected on the temperature dependence of  $g_{\perp}$  as well.

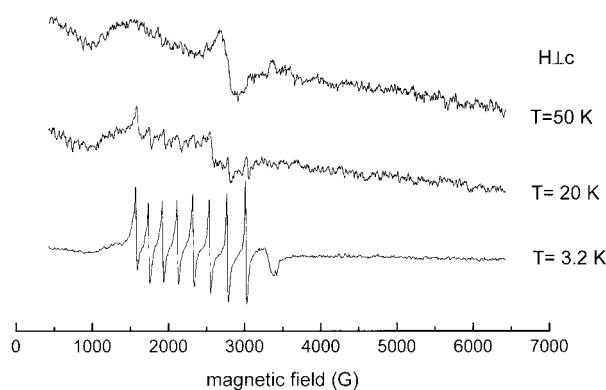


**Figure 1.** Hyperfine structure of the ESR signal of  $\text{Co}_{0.01}\text{Ni}_{0.99}\text{Pc}(\text{AsF}_6)_{0.5}$  at 3.2 K. Above 40 K, in a metallic phase, this hyperfine structure collapse into a single Lorentzian through the exchange coupling with itinerant  $\pi$ -electrons.

#### IV-A-2 Pressure-Temperature Phase Diagram of $\text{NiPc}(\text{AsF}_6)_{0.5}$

SIMONYAN, Mkhitar; YAKUSHI, Kyuya

We have shown before that  $\text{NiPc}(\text{AsF}_6)_{0.5}$  shows a continuous charge transfer from the metal 3d-band to the ligand  $\pi$ -band and this charge transfer begins at 1 GPa.<sup>1,2)</sup> From the analysis of the plasmon absorption band, we predicted that a metal-insulator (MI) transition accompanied this continuous charge transfer phenomenon. It is therefore expected that the MI transition occurs at the same pressure, *ca.* 1 GPa, at room temperature. On the other hand this compound undergoes a MI transition around 40 K at ambient pressure. This observation suggests that the temperature of this MI transition will increase from 40 K to room temperature when the high-pressure is applied to this compound. Figure 1 actually realizes our expectation: the resistance minimum monotonously increases up to 283 K at 0.95 GPa. The insulator phase of  $\text{NiPc}(\text{AsF}_6)_{0.5}$  brought about by the 3d- $\pi$  charge transfer is likely to be a state of Anderson localization. The mechanism of this MI transition is unique among the organic conductors.

#### References

- 1) T. Hiejima and K. Yakushi, *J. Chem. Phys.* **103**, 3950 (1995).
- 2) Y. Yonehara and K. Yakushi, *Synth. Met.* **94**, 149 (1998).

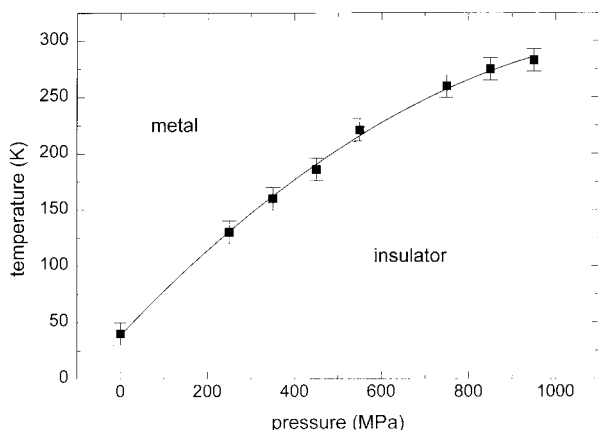


**Figure 1.** P-T Phase diagram of NiPc(AsF<sub>6</sub>)<sub>0.5</sub>: The squares represent the resistivity-minimum temperature against the pressure. Note that the insulator phase expands according to the pressure, which is associated with the continuous charge-transfer phenomenon.

#### IV-A-3 New Raman Bands Found in the Mixed Crystals of Ni<sub>1-x</sub>Co<sub>x</sub>Pc(AsF<sub>6</sub>)<sub>0.5</sub>

YONEHARA, Yukako<sup>1</sup>; DING, Yuqin<sup>1</sup>; SIMONYAN, Mkhitar; YAKUSHI, Kyuya  
(<sup>1</sup>GUAS)

We show by X-ray diffraction and EPMA that the nearly isostructural NiPc(AsF<sub>6</sub>)<sub>0.5</sub> and CoPc(AsF<sub>6</sub>)<sub>0.5</sub> make mixed crystals Ni<sub>1-x</sub>Co<sub>x</sub>Pc(AsF<sub>6</sub>)<sub>0.5</sub> in a wide range of  $x$  ( $1 \geq x \geq 0$ ). We find new Raman bands at 370 cm<sup>-1</sup> and 740 cm<sup>-1</sup> that appear only in the mixed crystals, when the He-Ne laser (632.8 nm) is polarized parallel to the  $c$ -axis (conducting axis). The symmetry of these Raman modes is a<sub>1g</sub>, since they appear in the configuration of  $b(c,c)-b$  or  $a(c,c,-)a$ . When we change the excitation light to Ar<sup>+</sup> laser (514.5 nm), these new Raman bands are remarkably weakened or disappear. This suggests the resonance effect for the appearance of the new bands, thereby new excited state is formed around  $15 \times 10^3$  cm<sup>-1</sup> in the mixed crystals and the transition moment to this excited state is parallel to the  $c$ -axis. This excited state is proposed to be a charge-transfer state from the filled 3d<sub>z<sup>2</sup></sub>-orbital of NiPc to the partly vacant 3d<sub>z<sup>2</sup></sub>-orbital of CoPc. The 370 cm<sup>-1</sup> and its overtone mode 740 cm<sup>-1</sup> are associated with the deformation mode of isoindole ring.

## IV-B Structure and Properties of Organic Conductors

The study of organic metals rapidly developed when the dimensionality of an intermolecular charge-transfer interaction is expanded. This expansion of dimensionality has been brought about by the discovery of new molecules such as BEDT-TTF or C<sub>60</sub>. The most basic physical parameters are the transfer integrals that represent the dimensionality and itinerancy of the electron, and the on-site Coulomb energy and coupling constants with molecular vibration, which represent the localized character of the electron. We systematically determine these parameters by polarized reflection spectroscopy assembling a microscope, multi-channel detection system, FT-IR, and liquid helium cryostat.

Another ongoing program is to look for negative- $U$  organic charge-transfer compounds, the strategy of which is described in the special research project of this issue. In this research program, the most important parameter is the charge or valence of the molecule in a mixed-valent state. The examination of the electronic and vibrational spectra at low temperature or high pressure is most efficient to characterize the valence. Molecular metals consisting of large or long molecules are examined by reflection and Raman spectroscopy at low temperature.

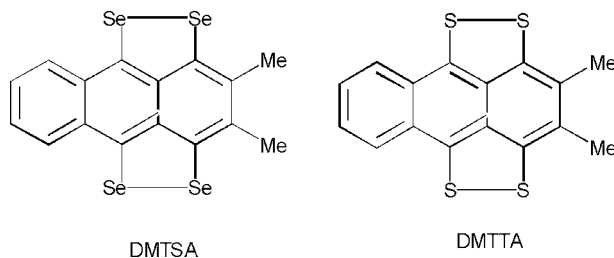
#### IV-B-1 Spectroscopic Study of Isostructural Charge-Transfer Salts: Non-Metallic DMTTA-BF<sub>4</sub> and Metallic DMTSA-BF<sub>4</sub>

OUYANG, Jianyong<sup>1</sup>; DONG, Jian<sup>1</sup>; YAKUSHI, Kyuya; TAKIMIYA, Kazuo<sup>2</sup>; OTSUBO, Tetsuo<sup>2</sup>  
(<sup>1</sup>GUAS; <sup>2</sup>Hiroshima Univ.)

[*J. Phys. Soc. Jpn.* in press]

We present the polarized reflection spectra of non-metallic DMTTA-BF<sub>4</sub> and the isostructural metallic DMTSA-BF<sub>4</sub>. From these spectra, both compounds were regarded as quasi-one-dimensional conductors. From the analysis of these spectra we show that DMTTA-BF<sub>4</sub> is a Mott insulator with  $U/4t \sim 0.8-1.2$  and DMTSA-BF<sub>4</sub> is a weakly correlated metal with structural fluctuation near the room temperature. Resistivity, thermopower, and ESR are consistent with the above picture, and demonstrate the phase transitions at *ca.* 100 K for DMTTA-BF<sub>4</sub> and at *ca.* 150 K for DMTSA-BF<sub>4</sub>. The low-temperature reflection spectra of

both compounds strongly suggest the breaking of screw-axis symmetry along the conducting axis. These phase transitions are regarded as the spin Peierls transition (DMTTA-BF<sub>4</sub>) and Peierls (DMTSA-BF<sub>4</sub>) transition. Assuming a dimerized stack, we estimate the transfer integrals  $t_1$  and  $t_2$  as 0.25 and 0.21 eV from the 10 K spectrum of DMTSA-BF<sub>4</sub>. The coupling constants of molecular vibration of DMTSA with the inter-molecular charge-transfer excitation are obtained analyzing the polarized reflection spectrum of DMTSA-ClO<sub>4</sub> having a dimerized structure.



#### IV-B-2 Suppression of the Metal-Insulator Transition under High Pressure in 1:1 Metallic DMTSA-BF<sub>4</sub>

SIMONYAN, Mkhitar; YAKUSHI, Kyuya; TAKIMIYA, Kazuo<sup>1</sup>; OTSUBO, Tetsuo<sup>1</sup>  
(<sup>1</sup>Hiroshima Univ.)

DMTSA-BF<sub>4</sub> undergoes a metal-insulator transition of a Peierls type.<sup>1)</sup> This phase transition is suppressed by applying 400 MPa as shown in the figure. Probably the inter-chain transfer integral  $t_{ab}$  is enhanced by the high pressure. Taking  $t_{ab}$  into account, we have examined the band structure of this compound. However, this transfer integral provides no change in one-dimensional Fermi surface, if the band is half-filled. The high-pressure experiment requires the further examination of the band-filling factor or inter-chain coupling through the counter anion BF<sub>4</sub>.

We have measured the resistance of 500 MPa down to 0.23 K using the <sup>3</sup>He cryostat equipped in the Molecular Materials Center. However, superconductivity was not found in this compound at this pressure. All organic compound which shows superconductivity has TTF skeleton. This might suggest that the high-frequency phonon structure is associated with the mechanism of the superconductivity in organic superconductor.

#### Reference

1) J. Dong, K. Yakushi, K. Takimiya and T. Otsubo, *J. Phys. Soc. Jpn.* **67**, 971 (1998).

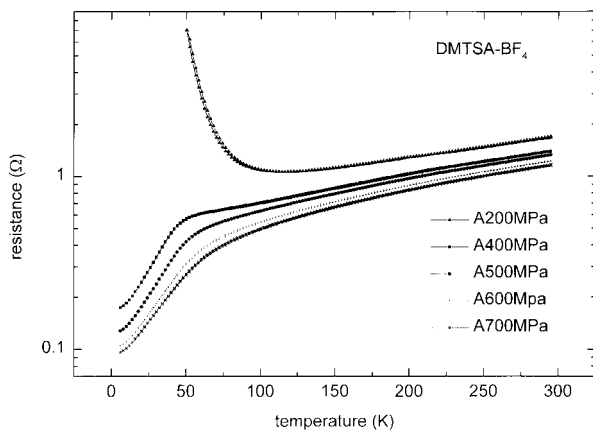


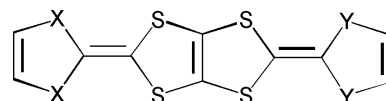
**Figure 1.** Temperature dependence of the resistance of DMTSA-BF<sub>4</sub>. The metallic state is maintained at least down to 2 K above 400 MPa.

#### IV-B-3 Band Structure of Organic Metals (BDT-TTP)<sub>2</sub>X (X = ClO<sub>4</sub>, ReO<sub>4</sub>), (ST-TTP)<sub>2</sub>AsF<sub>6</sub>, and (BDS-TTP)<sub>2</sub>AsF<sub>6</sub> Studied by Reflection Spectroscopy

OUYANG, Jianyong<sup>1</sup>; YAKUSHI, Kyuya; MISAKI, Yohji<sup>2</sup>; TANAKA, Kazuyoshi<sup>2</sup>  
(<sup>1</sup>GUAS; <sup>2</sup>Kyoto Univ.)

The charge-transfer salts of BDT-TTP with  $\beta$ -type molecular arrangement have quasi-one-dimensional metallic band. We have experimentally determined the

intra ( $t_a$ )- and inter-chain ( $t_p$ ) transfer integrals of (BDT-TT)<sub>2</sub>X (X = AsF<sub>6</sub>, SbF<sub>6</sub>)<sub>0.5</sub>. We apply the same spectroscopic method to the title compounds. (ST-TTP)<sub>2</sub>AsF<sub>6</sub> and (BDS-TTP)<sub>2</sub>AsF<sub>6</sub> are isostructural to (BDT-TTP)<sub>2</sub>SbF<sub>6</sub> with P1 space group. The transfer integrals are  $t_a = -0.24$  eV,  $t_p = -0.042$  eV for (ST-TTP)<sub>2</sub>AsF<sub>6</sub> and  $t_a = -0.26$  eV,  $t_p = -0.044$  eV for (BDS-TTP)<sub>2</sub>AsF<sub>6</sub>. These values are not significantly enhanced compared with (BDT-TTF)<sub>2</sub>X (X = AsF<sub>6</sub>, SbF<sub>6</sub>), although selenium atoms are introduced at the outer sulfur position. Probably the increase of the overlap between selenium-sulfur orbitals is compensated by the decrease of the sulfur-sulfur overlap. This system became more anisotropic at low temperatures as well as (BDT-TTF)<sub>2</sub>X (X = AsF<sub>6</sub>, SbF<sub>6</sub>). (BDT-TTP)<sub>2</sub>X (X = ClO<sub>4</sub>, ReO<sub>4</sub>) are isostructural to each other with the space group of C2/c. The intra-chain ( $t_b$ ) and inter-chain ( $t_p$ ) transfer integrals are estimated as  $t_b = 0.26$  eV,  $t_p = -0.048$  eV for ClO<sub>4</sub> salt and  $t_b = 0.25$  eV,  $t_p = -0.047$  eV for ReO<sub>4</sub> salt. From the spectral data we corrected the chemical ratio of ReO<sub>4</sub> salt as 2:1, although it was reported as (BDT-TTP)<sub>2</sub>(ReO<sub>4</sub>)<sub>0.72</sub>. We analyze the reflectivity curve  $R(\omega)$  using generalized Drude model and find  $R(\omega)$  along the inter-chain direction deviates significantly from the simple Drude model.



X = Y = S: BDT-TTP  
X = S, Y = Se: ST-TTP  
X = Y = Se: BDS-TTP

#### IV-B-4 Insulator-Insulator Phase Transition of $\theta$ -(BDT-TTP)<sub>2</sub>Cu(NCS)<sub>2</sub>: Strongly Correlated Two-Dimensional System

OUYANG, Jianyong<sup>1</sup>; YAKUSHI, Kyuya; MISAKI, Yohji<sup>2</sup>; TANAKA, Kazuyoshi<sup>2</sup>  
(<sup>1</sup>GUAS; <sup>2</sup>Kyoto Univ.)

Contrary to the metallic properties of  $\beta$ -type (BDT-TTP)<sub>2</sub>X,  $\theta$ -type (BDT-TTP)<sub>2</sub>Cu(NCS)<sub>2</sub> is an insulator, although a simple tight-binding calculation leads to a two-dimensional metallic band. A phase transition is found at 250 K in the electrical resistance measurement, the activation energy being changed from 30-40 meV (HT phase) to 100 meV (LT phase). The spin susceptibility changes the temperature dependence at 250 K, below which it conforms to a Curie-Weiss law with  $C = 0.143$  and  $\theta = 19$  K. Although this magnetic property is not well understood, it is safely concluded that the charge on BDT-TTP is rather localized in the LT phase. The reflectivity exhibits the so-called charge-transfer (CT) band in two polarization directions, which means the inter-molecular interaction is two-dimensional. This CT band dramatically changes at the phase transition temperature, increasing the gap energy below the phase transition temperature. This behavior strongly suggests the structural change through the phase transition, although the LT phase structure is not known. As shown in the figure, the Raman spectrum of the C=C stretching mode has an asymmetric broad lineshape in HT phase.

It shows a complicated splitting accompanied by the appearance of new peaks below the phase transition temperature. This splitting may be associated with the charge disproportionation.

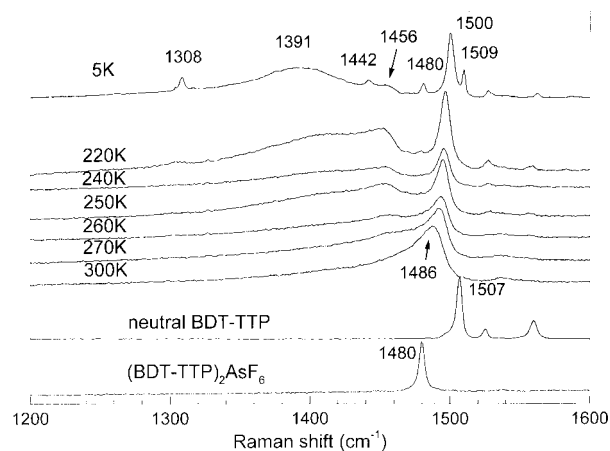


**Figure 1.** Temperature dependence of the Raman spectrum of C=C stretching mode in  $\theta$ -(BDT-TTP)<sub>2</sub>Cu(NCS)<sub>2</sub> along with the room-temperature spectrum of BDT-TTP and (BDT-TTP)<sub>2</sub>AsF<sub>6</sub> crystals. This charge-sensitive mode continuously changes during the phase transition.

#### IV-B-5 Phase Transition in Narrow-band Organic Metals (BEDT-ATD)<sub>2</sub>X(solvent) (X = PF<sub>6</sub>, AsF<sub>6</sub>, BF<sub>4</sub>; solvent = THF, DHF, DO)

YAKUSHI, Kyuya; URUICHI, Mikio; YAMASHITA, Yoshiro

[*Synth. Met.* in press]

We present the metal-insulator (MI) transition of the title compounds examined by reflection spectroscopy, X-ray diffraction, and magnetic susceptibility. Below the MI transition temperature, the space group changes from  $P2_1/a$  to  $Pa$  with  $4k_F$  lattice modulation in (BEDT-ATD)<sub>2</sub>PF<sub>6</sub>(DHF) and (BEDT-ATD)<sub>2</sub>BF<sub>4</sub>(THF) which undergo MI transitions at 150 K and 200 K, respectively. On the other hand, the symmetry change is not observed at about 80 K in (BEDT-ATD)<sub>2</sub>PF<sub>6</sub>(DO) ( $T_{MI} = 100$  K), (BEDT-ATD)<sub>2</sub>PF<sub>6</sub>(THF) ( $T_{MI} < 50$  K), and (BEDT-ATD)<sub>2</sub>AsF<sub>6</sub>(THF) ( $T_{MI} < 50$  K). The  $4k_F$  lattice modulation is supported by the magnetic susceptibility experiment as well. The precursor phenomenon of this structural change is observed already at room temperature in (BEDT-ATD)<sub>2</sub>PF<sub>6</sub>(DO). All of these data suggest the view that (BEDT-ATD)<sub>2</sub>X(solvent) is a strongly correlated 1D metal.

The breaking of the center of symmetry in several solvent-containing crystals requires that asymmetric solvents are aligned ferroelectrically below the MI transition temperature as shown in the figure. This suggests the possibility of the ferroelectric state just below the phase transition temperature. The experiment to examine this unusual possibility is now in progress.

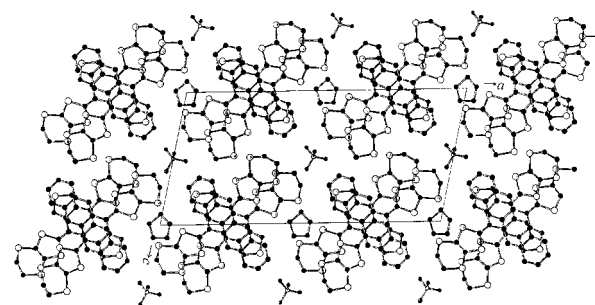
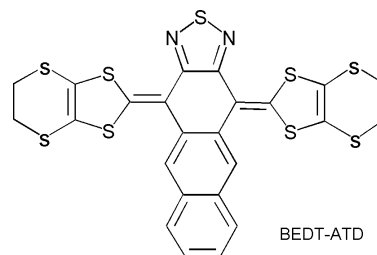


**Figure 1.** Low-temperature crystal structure of (BEDT-ATD)<sub>2</sub>BF<sub>4</sub>(THF).

#### IV-B-6 Experimental and Theoretical Estimation of the Site-Energy Difference in Et<sub>4</sub>N(DMTCNQ)<sub>2</sub>

NAKANO, Chikako; YAKUSHI, Kyuya; UEDA, Kazushi<sup>1</sup>; SUGIMOTO, Toyoshige<sup>1</sup>  
(<sup>1</sup>Osaka Pref. Univ.)

[*Chem. Phys. Lett.* in preparation]

DMTCNQ forms a dimerized stack in (Et<sub>4</sub>N)-(DMTCNQ)<sub>2</sub> with two crystallographically independent sites. Although the average charge of DMTCNQ is  $-0.5$ , the charge in different site has a different value such as  $-0.5 + \delta$  and  $-0.5 - \delta$ . We have estimated this  $\delta$  as 0.1 by the Raman spectroscopy. The different charge on the non-equivalent site comes from the site-energy difference in the unit cell. This kind of charge disproportionation is sometimes accompanied by the phase transition in organic conductors such as (DI-DCNQI)<sub>2</sub>-Ag and  $\alpha'$ -(BEDT-TTF)<sub>2</sub>IBr<sub>2</sub> and is attracting an attention as a new ground state. The pattern of the charge distribution is not only determined by the repulsive force between the adjacent localized charges but also by the electrostatic force with counter anion/cation. Following the last year's experimental work, we conducted the numerical calculation of the Madelung energy, which brings about the site-energy difference. We first calculate the charge distribution in DMTCNQ<sup>0</sup>, DMTCNQ<sup>-</sup>, and Et<sub>4</sub>N<sup>+</sup> using the PM3 semi-empirical method in the HyperChem-R5.1 program system. The infinite sum of the electrostatic energy between these point charges is calculated using the Ewald method. The site-energy difference is calculated as 0.14 eV. On the other hand, this site energy difference is estimated based on the ion-neutral dimer model analyzing the reflection and Raman spectra. It is experimentally estimated as 0.082 eV. The agreement with numerical estimation is satisfactory.

#### IV-B-7 $\kappa'$ -(ET)<sub>2</sub>Cu<sub>2</sub>(CN)<sub>3</sub>—Superconductor with Mixed Cu<sub>2</sub>(CN)<sub>3</sub> and N(CN)<sub>2</sub> Ligands in the Anion Layer Studied by Polarized Reflection Spectroscopy

DROZDOVA, Olga<sup>1</sup>; YAKUSHI, Kyuya; SAITO, Gunzi<sup>1</sup>; OOKUBO, Kenji<sup>1</sup>; YAMOCHI, Hideki<sup>1</sup>; KONDO, Tetsuo; URUICHI, Mikio; OUAHAB, Lahcène<sup>2</sup>

(<sup>1</sup>Kyoto Univ.; <sup>2</sup>Univ. Rennes)

Since the first discovery of (ET)<sub>2</sub>Cu<sub>2</sub>(CN)<sub>3</sub> with  $\kappa$ -type donor packing, controversial results were reported concerning its conducting properties. “ $\kappa$ ” Abbreviation was introduced to distinguish an ambient pressure superconductor with  $T_c = 3.8$  K from the semiconductor “ $\kappa'$ ” with  $E_a = 0.04$ – $0.05$  eV. The same preparation conditions give the 11.2 K superconductor  $\kappa$ -(ET)<sub>2</sub>Cu(CN)[N(CN)<sub>2</sub>]. Polarized reflection spectra were measured on the conductive (*bc*) plane of  $\kappa$ -(ET)<sub>2</sub>Cu<sub>2</sub>(CN)<sub>3</sub>,  $\kappa'$ -(ET)<sub>2</sub>Cu<sub>2</sub>(CN)<sub>3</sub> and  $\kappa$ -(ET)<sub>2</sub>Cu(CN)-[N(CN)<sub>2</sub>]. Despite the overall similarity of the spectra at 293 K, clear difference in the 2100–2300 cm<sup>-1</sup> range was observed. Namely,  $\kappa'$ -(ET)<sub>2</sub>Cu<sub>2</sub>(CN)<sub>3</sub> exhibits CN stretching peaks characteristic for both  $\kappa$ -(ET)<sub>2</sub>Cu<sub>2</sub>(CN)<sub>3</sub> and  $\kappa$ -(ET)<sub>2</sub>Cu(CN)[N(CN)<sub>2</sub>]. Thus anion layer of  $\kappa'$  is regarded as mixture of Cu<sub>2</sub>(CN)<sub>3</sub> and Cu(CN)-[N(CN)<sub>2</sub>] anions. The mixing ratio was estimated as 2:1 in most samples. Angle dependence suggested that the orientation of the original features conserved within the anion layer of  $\kappa'$ . Homogeneity of the mixing was supported by Raman spectroscopy. Temperature evolution of the reflection spectra followed conducting properties. The chemical formula of  $\kappa'$ -(ET)<sub>2</sub>Cu<sub>2</sub>(CN)<sub>3</sub> was modified to  $\kappa$ -(ET)<sub>2</sub>Cu<sup>+(2-x-y)</sup>Cu<sup>2+x</sup>(CN)<sub>(3-2y)</sub>-[N(CN)<sub>2</sub>]<sub>y</sub>, where  $x < 0.01$  and  $0.1 \leq y \leq 0.8$ .

#### IV-B-8 Raman-active C=C Vibrations of $\kappa$ -(BEDT-TTF)<sub>2</sub>Cu[N(CN)<sub>2</sub>]Br and Its Deuterated Analogues

MAKSIMUK, Mikhail; YAKUSHI, Kyuya; KAWAMOTO, Atsushi<sup>1</sup>; TANIGUCHI, Hiromi<sup>2</sup>; KANODA, Kazushi<sup>2</sup>

(<sup>1</sup>Hokkaido Univ.; <sup>2</sup>Tokyo Univ.)

The set of progressively deuterated isotopic analogues of  $\kappa$ -(BEDT-TTF)<sub>2</sub>Cu[N(CN)<sub>2</sub>]Br lies on the border between metals and insulators. Below 80 K, a crystal volume is divided into a metallic phase and an insulating one. The amount of the latter increases with deuteration and depends on the cooling rate near 80K. These crystals have several anomalies in temperature dependencies of their various physical properties. We studied d[0,0], d[2,2], d[3,3] and d[4,4] single crystals, the numbers being the numbers of deuterium atoms in every end of a BEDT-TTF molecule. The C=C stretching modes in resonance Raman spectra (laser wavelength 514.5 nm) have been measured at temperatures between 4.2 and 300 K. In d[2,2], d[3,3] and d[4,4], four modes have been observed: well-known totally symmetric  $\nu_2$ ,  $\nu_3$ ; vibronically coupled  $\nu_{27}^-(B_{1u})$  and a mode near 1463 cm<sup>-1</sup> (at 5 K) which we assign to  $\nu_{27}^+(B_{1u})$ . In d[0,0] below 200K, in addition to that, it

has been possible to resolve dimer-dimer splitting of  $\nu_2$  and  $\nu_3$ .  $\nu_2$  and  $\nu_3$  have different temperature dependence of this splitting. In d[2,2] all  $\nu_{27}^-$  parameters and the width of  $\nu_2$  depend on the cooling rate near 80 K as well as they are sample-dependent. In both cases it can be explained as the influence of the electronic system: for  $\nu_{27}^-$  by electron-molecular vibration coupling and for  $\nu_2$  width by a change of the dimer-dimer splitting.

#### IV-B-9 Determination of the Charge on BEDO-TTF in Its Complexes by Raman Spectroscopy

DROZDOVA, Olga<sup>1</sup>; YAMOCHI, Hideki<sup>1</sup>; YAKUSHI, Kyuya; URUICHI, Mikio; HORIUCHI, Sachio; SAITO, Gunzi<sup>1</sup>

(<sup>1</sup>Kyoto Univ.)

[*J. Am. Chem. Soc.* submitted]

Raman spectroscopy was employed as a fast and exact method to determine the charge on BEDO-TTF (BO) in its complexes. Linear dependencies between two totally symmetric C=C stretching modes ( $\nu_2$ : ring C=C and  $\nu_3$ : central C=C) and charge on BO were found and used to evaluate the charge transfer (CT) degree. The CT degree was evaluated by the following equation.

$$\rho = (1524.9 - \nu_{3,obs}(\text{cm}^{-1}))/109.0$$

$$\rho = (1660.8 - \nu_{2,obs}(\text{cm}^{-1}))/74.1$$

Using the above equation, 19 complexes, including single crystals, powders and films were examined for the first time. The border between neutral (insulating) and partially CT (conducting) complex based on BO was estimated as 0.3.

#### IV-B-10 Re-examination of Bromide, Chloride and Iodide Salts of Bis(ethylenedioxy)tetra-thiafulvalene (BEDO-TTF) by Spectroscopic Methods

ULANSKI, Jacek; YAKUSHI, Kyuya; URUICHI, Mikio; DROZDOVA, Olga<sup>1</sup>; YAMOCHI, Hideki<sup>1</sup>; SAITO, Gunzi<sup>1</sup>

(<sup>1</sup>Kyoto Univ.)

[*J. Phys. B: Condens. Matter* in preparation]

Recent results of polarized reflectivity, absorption and Raman spectroscopic studies of (BEDO-TTF)<sub>2</sub>Br·(H<sub>2</sub>O)<sub>3</sub>, (BEDO-TTF)<sub>2</sub>·4I<sub>3</sub>, and (BEDO-TTF)<sub>2</sub>Cl·(H<sub>2</sub>O)<sub>3</sub> salts are summarized and analyzed. The experimentally obtained plasma frequencies and transfer integrals are considerably smaller than the theoretical values calculated including 3d orbitals; the theoretical calculations neglecting the sulfur 3d orbitals yield more realistic band structure. The polarized reflectance and optical conductivity spectra of the investigated BEDO-TTF salts in the direction perpendicular to the conducting plane reveal some unique features: very strong vibrational bands which originate from vibrations of BEDO-TTF molecules, and in some cases new bands around 5000 cm<sup>-1</sup> due to directional dispersion. Detailed analysis of the bands in the range 3200–3500 cm<sup>-1</sup> shows that the compositions of the chloride and of

the bromide salts are still not clear in respect to possible presence of the hydroxonium ions and to the role of water molecules. The BEDO-TTF salts containing water molecules are not stable in vacuum, losing both water and anion molecules, what should be taken into account in further investigations of these materials. The absorption spectra for thin, semitransparent single crystal of BEDO-TTF bromide salt, taken at different angles of incident light, demonstrate that the high transparency is due to specific orientation of the BEDO-TTF molecules.

#### IV-B-11 First Observation of the Plasmon Absorption by Reflection Spectroscopy in the Single Crystal of Two-dimensional Organic Metal

YAKUSHI, Kyuya; ULANSKI, Jacek; YAMOCHI, Hideki<sup>1</sup>; SAITO, Gunzi<sup>1</sup>  
(<sup>1</sup>Kyoto Univ.)

Plasmon cannot be detected by the optical absorption method, since it is a longitudinal excitation. However, it becomes detectable in an anisotropic material, if the wave vector of light is not parallel to the principal axis of the anisotropic material. We present the observation and simulation of the plasmon by the method of normal incidence reflection spectroscopy in two-dimensional organic metals  $\text{BO}_2\text{Cl}(\text{H}_2\text{O})_3$  and  $\text{BO}_{2.4}\text{I}_3$ . The plasmon was observed in the specular reflection normal to (111) and  $(11\bar{1})$  crystal faces, which respectively make angles of  $71.0^\circ$  and  $78.7^\circ$  with conducting sheet in  $\text{BO}_2\text{Cl}(\text{H}_2\text{O})_3$ , and that to the  $(\bar{1}01)$  crystal face, which makes an angle of  $67.0^\circ$  with the conducting sheet in  $\text{BO}_{2.4}\text{I}_3$ . The plasmon spectrum is theoretically reproduced solving the Fresnel equation with the principal dielectric function for a two-dimensional metal. We have given the analytical solution of the two-dimensional case. In both cases, the theoretical prediction agrees very well with the observation of the reflectivity at each crystal face. This is the first observation of the plasmon in organic metals. Incidentally, this is physically the same phenomenon as the directional dispersion in an exciton absorption of organic dye.

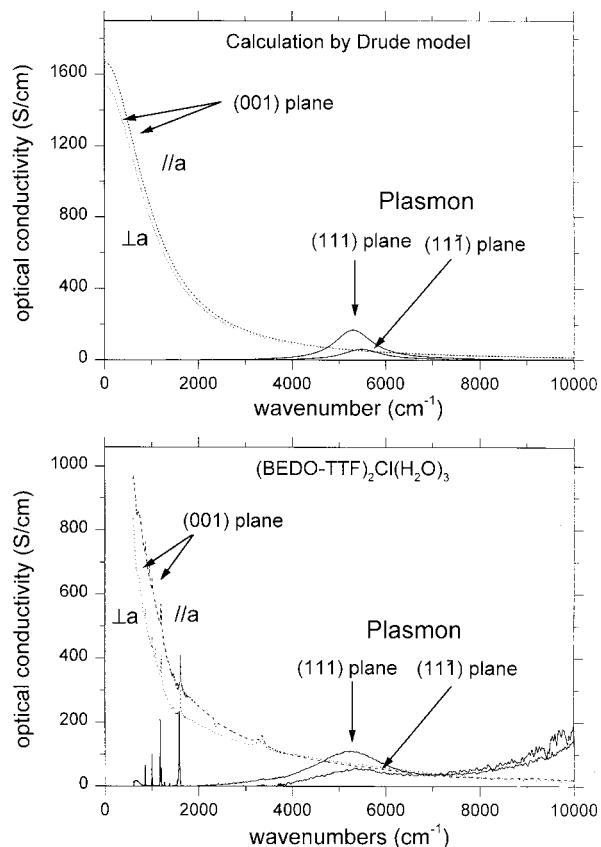


**Figure 1.** Observed and calculated conductivity spectra in the principal directions //a and  $\perp a$  on the (001) conducting plane and non-principal directions on (111) and  $(11\bar{1})$  plane in the crystal of  $\text{BO}_2\text{Cl}(\text{H}_2\text{O})_3$ . Plasmon peak appears at  $5000\text{--}6000\text{ cm}^{-1}$  in the spectra on the (111) and  $(11\bar{1})$  planes.